Available online at www.sciencedirect.com
SCIENCE DIRECT
Polymer 46 (2005) 9702–9713
polymer
www.elsevier.com/locate/polymer

The effects of clay on the thermal degradation behavior of poly(styrene-*co*-acrylonitirile)

Bok Nam Jang, Charles A. Wilkie*

Department of Chemistry, Marquette University, P.O. Box 1881, Milwaukee, WI 53201 USA

Received 5 May 2005; received in revised form 21 July 2005; accepted 26 July 2005
Available online 10 August 2005

Abstract

The thermal degradation of poly(acrylonitrile-*co*-styrene) (SAN) and its clay nanocomposites were studied using TGA/FTIR and GC/MS. Virgin SAN degrades by chain scission followed by β-scission, producing monomers, dimers and trimers. The degradation pathway of SAN in clay nanocomposites contains additional steps; extensive random chain scission, evolving additional compounds having an odd number of carbons in the chain backbones, and radical recombination, producing head-to-head structures. Since acrylonitrile-butadiene-styrene copolymer (ABS) has butadiene rubber incorporated as a grafted phase in a SAN matrix, ABS follows a similar degradation pathway as that of SAN. The effect of butadiene rubber is similar to that of clay, leading to extensive random scission and an increase in thermal stability, but as not effective as clay due to its shorter duration. Eventually, the butadiene rubber phase degrades to small aliphatic molecules.

Keywords: SAN; Thermal degradation; Nanocomposites

1. Introduction

Polymer/clay nanocomposites offer the advantage of a large interfacial area and good compatibility between the nano-dimensional material and the polymer, which leads to increased mechanical [1–3], barrier [4] and fire properties [5–8]. The introduction of polymer/clay nanocomposites have attracted considerable attention from an application point of view [9,10] since the addition of a small amount of clay ($\leq$5 wt%) leads to a large enhancement of the properties indicated above.

The formation of well-dispersed polymer nanocomposites also leads to modification of the degradation pathway of polymers and this clearly affects the fire behavior of nanocomposites. The currently accepted explanation for enhanced fire properties is that the clay forms a barrier to mass transport and which also insulates the underlying polymer from the heat source [11]. For example, the clay nanocomposites of polystyrene [12], polyamide 6 [13] and poly(ethylene-*co*-vinylacetate) [14] exhibit a 60% reduction in the peak heat release rate (PHRR) in the cone calorimeter experiment. In this laboratory, GC/MS, as well as TGA/FTIR, has been used to study the degradation pathway of the clay nanocomposites of the above polymers and it has been shown that inter-chain reactions, such as radical recombination, are an important addition to the degradation pathway of the virgin polymers, and this is due to the barrier effect of the clay. Thus, the chains fragmented during thermal degradation are momentarily contained between the clay layers and this permits inter-chain reactions. A similar containment of degrading polymers by clay has also been reported by Vyazovkin for polystyrene nanocomposites [15].

Copolymers are increasingly important industrially because the introduction of one component may make up for shortcomings due to the other component. One representative copolymer is poly(styrene-*co*-acrylonitrile) (SAN), which exhibits the combined properties of the ease of processing of polystyrene and the rigidity and chemical resistance of polyacrylonitrile. Acrylonitrile-butadiene-styrene terc (ABS) incorporates butadiene rubber into SAN, which imparts high impact strength to the copolymer. Thus, SAN and ABS are widely used in a variety of industrial applications due to good mechanical properties, chemical resistance and ease of processing.

* Corresponding author.
E-mail address: charles.wilkie@marquette.edu (C.A. Wilkie).

0032-3861/$ - see front matter © 2005 Elsevier Ltd. All rights reserved.
doi:10.1016/j.polymer.2005.07.078

Since ABS consists of a SAN matrix embedded with butadiene rubber particles, the degradation of ABS is closely related to the degradation behavior of SAN. For the study of thermal degradation or fire retardancy of ABS systems, SAN is used as a model to simplify the system [16]. The thermal degradation of SAN copolymer was studied by Grassie and Bain [17–19] using thermal volatilization analysis (TVA) and GC/MS. They proposed that a depolymerization for the SAN copolymer is the main degradation pathway, similar to that in polystyrene. Regarding the thermal degradation pathway of ABS, it was shown that the degradation pathway follows the same depolymerization pathway and the products that can be assigned by GC/MS are mainly from the degradation of the SAN phase in ABS [20–22].

Clay nanocomposite formation using SAN or ABS as a polymer matrix brings about improvement in mechanical strength and fire retardancy [14,23]. Since some changes occur in the degradation of polystyrene nanocomposite compared to virgin polystyrene [12], this study is designed to determine if similar changes are also seen for SAN and ABS. Because the primary difference between ABS and SAN is the presence of butadiene rubber, the effect of butadiene rubber on the thermal stability and degradation pathway of ABS is also explored in this study.

2. Experimental

2.1. Organically modified clays

Three different organically-modified monmorillonite clays were used; 30B-clay (Cloisite 30B, 70% clay and 30% methyl hydrogenated tallow bis(2-hydroxyethyl) ammonium) and 10A-clay (Cloisite 10A, 70% clay and 30% dimethylbenzyl hydrogenated tallow ammonium) were supplied by Southern Clay Products, Inc., while Np-clay (70% clay and 30% dimethyl naphthenatehexadecyl ammonium) was prepared following the literature procedure [24]. The structures of ammonium cations used for the modification of clay are shown in Fig. 1.

2.2. Preparation of SAN/clay and ABS/clay nanocomposites

Poly(styrene-*co*-acrylonitrile) (SAN) and acrylonitrile-butadiene-styrene terpolymer (ABS) were provided by Cheil Industries Inc.; the mass ratio of styrene/acrylonitrile in SAN is 75/25 (mole ratio: 60.4/39.6) and the butadiene rubber content in ABS is 17 wt%. SAN and ABS polymers were melt-blended with 30B-clay, 10A-clay and Np-clay in a Brabender Mixer at 60 rpm for 10 min at 200–210 °C. The inorganic clay content for all SAN or ABS/clay nanocomposites is 5.0 wt%, but TEM images were taken at 3.0 wt% inorganic clay content. To see the effect of the butadiene rubber on the thermal degradation of the SAN matrix, samples having 5.0 and 10% butadiene rubber content in the SAN matrix were prepared by controlling the mixing ratios between SAN and ABS appropriate to obtain these butadiene contents.

2.3. Characterization of the nanocomposites

X-ray diffraction (XRD), cone calorimetry and transmission electron microscopy (TEM) were used to characterize the dispersion of clay and the formation of nanocomposites. XRD patterns were obtained using a Rigaku Geiger Flex, 2-circle powder diffractometer equipped with Cu Kα generator ($\lambda = 1.5404$ Å); generator tension was 50 kV and the current was 20 mA. Cone calorimetry was performed on an Atlas CONE2 according to ASTM E 1354 at a heat flux of 35 kW/m^2, using a cone shaped heater. The exhaust flow rate was 24 l/s and the spark was continuous until the sample ignited. The specimens for cone calorimetry were prepared by the compression molding of the sample (about 30 g) into $3 \times 100 \times 100$ mm^3 square plaques. Typical cone calorimetry results are reproducible within $\pm 10\%$. TEM images were obtained at 60 kV with a Zeiss 10c electron microscope; the samples were microtomed at room temperature to give sections with a nominal thickness of 70 nm, using a Richert-Jung Ultra-Cut E microtome. Low-magnification and high-magnification images were taken at 10,000× and 50,000×, respectively.

2.4. TGA/FTIR analysis and sampling of the evolved products

TGA/FTIR was carried out on a Cahn TG 131 instrument, which was connected to a Mattson Research grade FTIR through a stainless steel tubing. The temperature reproducibility of the TGA is ± 3 °C and error range of non-volatile fraction at 600 °C is $\pm 3\%$. The thermal degradation in TGA was carried out at a heating rate of 20 °C/min and a nitrogen flow of 80 ml/min. The sample size was 40–60 mg for the TGA evaluation. During thermal

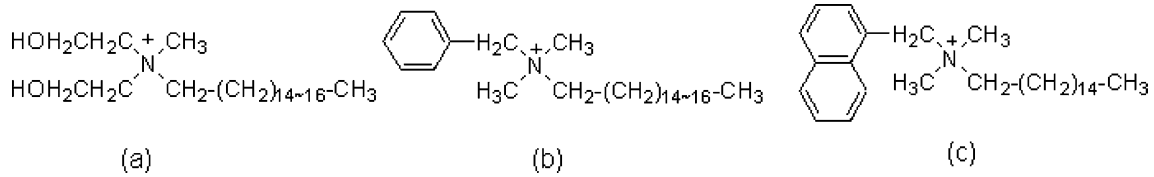

Fig. 1. Structures of the ammonium cations; (a) methyl hydrogenated tallow bis(2-hydroxyethyl) ammonium, 30B; (b) dimethyl benzyl hydrogenated tallow ammonium, 10A; and (c) dimethyl naphthenatehexadecyl ammonium, Np.

degradation in the TGA, the evolved volatile products are introduced to the IR chamber through a sniffer tube and stainless steel tubing and in situ vapor phase FTIR spectra are collected; this sniffer tube extends into the sample cup in the TGA and removes the evolved products at a rate of 40 ml/min. The temperature of the tubing was maintained at 300 °C. The evolved products during thermal degradation of each sample were collected using a cold trap at a temperature of −78 °C for the GC/MS analysis of the degradation products.

2.5. Analysis of the evolved condensable products

The collected evolved products in the trap were washed with acetonitrile and GC/MS spectra were obtained using an Agilent 6850 series GC connected to an Agilent 5973 Series MS (70 eV electron ionization) with temperature programming from 40 to 250 °C. The identities of evolved compounds were established by co-injection with authentic compounds and/or by the analysis of mass fragmentation pattern.

3. Results and discussion

3.1. The characterization of nanocomposite formation

The formation of a nanocomposite between SAN and ABS and modified clays was characterized by XRD, TEM and cone calorimetry. The XRD traces and TEM images of SAN have already been reported [25] and those of ABS are shown in Figs. 2 and 3. Both SAN and ABS nanocomposites have a *d*-spacing of 3.0 nm with all clays (the *d*-spacing in the organically-modified clays before nanocomposite formation ranges from 1.8 to 2.8 nm) [23], and ABS/Np clay shows a small peak at 5°, indicating some clay was not well mixed. TEM images show that the clay is well-dispersed and that an intercalated nanocomposite is formed.

The reduction in the peak heat release rate has been used as an indication of nanocomposite formation, since a microcomposite gives no reduction, while nanocomposites do show substantial reduction in the peak heat release rate [26,27]. Bourbigot and coworkers showed that SAN/clay nanocomposites, prepared by melt blending, exhibit good nano-dispersion at any clay loading up to 8% and the reduction in the peak heat release rate is proportional to the clay content [28]. Figs. 4 and 5 shows the cone results for SAN and ABS nanocomposites. The cone results show the same trend as observed in the XRD. A 45% reduct7ion in the PHRR for the both SAN and ABS samples using 10A-clay or 30B-clay is observed; similar results for SAN/clay nanocomposites prepared by melt-blending have been reported in the literature [26,29]. This 45% reduction in PHRR for SAN and ABS argues for good nano-dispersion, because this is comparable to the largest reductions that have been seen for these nanocomposites [26]. On the other hand, the SAN/Np-Clay nanocomposite shows a 20% reduction in PHRR and ABS/Np-clay exhibits a 35% reduction, which suggests that the nano-dispersion is not as good with this clay and this is supported by the weak intensity of the peaks and the small peak at 5° in the XRD traces for these materials. Since both 30B clay and 10A clay show the characteristics of well-dispersed clay nanocomposites, the 10A clay is utilized for the study of degradation of SAN and ABS nanocomposites.

3.2. The effect of butadiene rubber on the thermal stability of SAN and SAN nanocomposites

SAN is a random copolymer of styrene and acrylonitrile, while ABS contains an additional monomer, butadiene. ABS is usually prepared by the copolymerization of styrene and acrylonitrile in the presence of butadiene rubber particles which were pre-homopolymerized, and it consists of three phases; butadiene rubber, grafted SAN, and free SAN. The typical morphology of ABS consists of spherical butadiene rubber particles, which are surrounded by SAN that is grafted onto butadiene, and the continuous free SAN phase [30]. Thus, the main difference between SAN and ABS is the presence of butadiene rubber that was grafted by SAN. In this study, the effect of the rubber phase on the thermal and fire stability of SAN is explored.

Since ABS contains 17 wt% butadiene rubber which is evenly distributed in the SAN phase, samples with different rubber contents can be prepared through melt-blending by changing the ratio of ABS and SAN with and without organically-modified clay, for instance, the 'ABS-5R/clay' means that there is a 5 wt% of butadiene rubber in the ABS matrix and 5 wt% of inorganic clay (or 7 wt% of organically modified clay (10A clay)) is present in total composition.

The TGA results of the virgin polymers and their clay nanocomposites as a function of rubber content are shown in Figs. 6 and 7. The onset temperature, characterized as the temperature at which 10% degradation occurs, T_{10}, and the mid-point temperature of the degradation, another measure of thermal stability, T_{50}, as well as the fraction of material that is not volatile at 600 °C, denoted as char, are summarized in Table 1. As the rubber content in SAN increases, the thermal stability increases, and the

Table 1
TGA data for SAN and ABS and their nanocomposites

Sample	T_{10} (°C)	T_{50} (°C)	Residue at 600 °C (%)
SAN	419	442	1
SAN/clay	427	456	6
ABS-5R	424	447	1
ABS-5R/clay	423	454	6
ABS-10R	426	453	1
ABS-10R/clay	429	461	7
ABS-17R	420	454	3
ABS-17R/clay	429	463	6

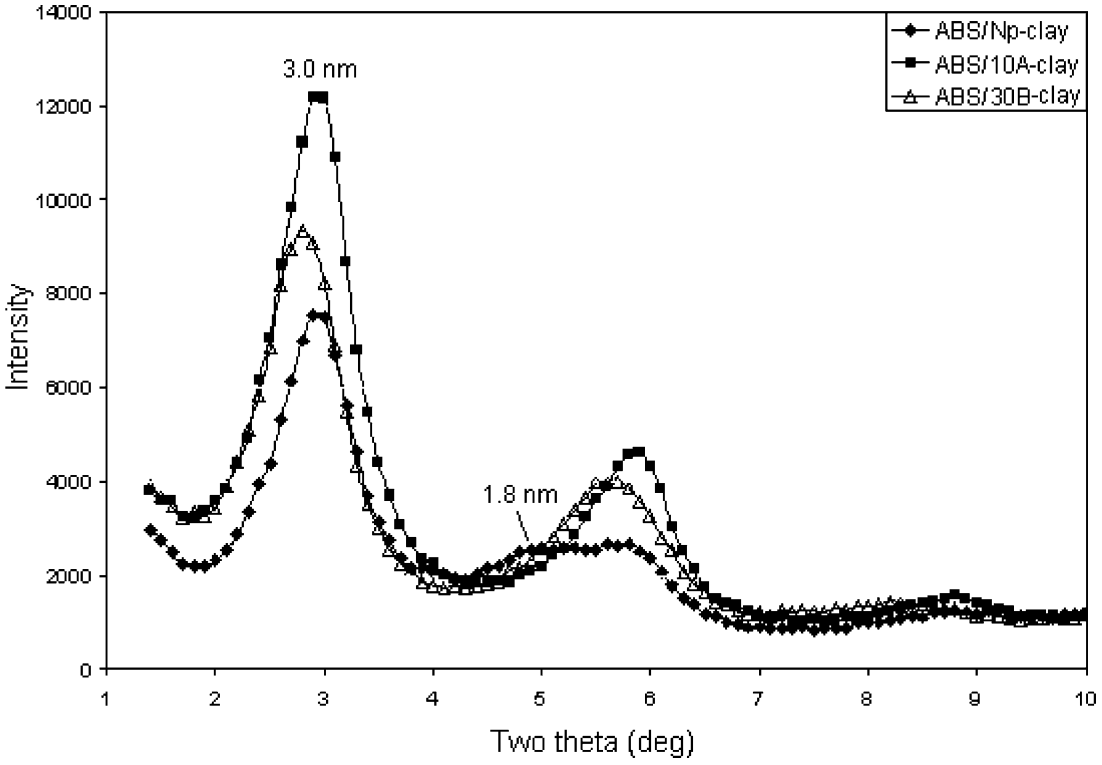

Fig. 2. XRD patterns for the ABS/clay having 5.0% inorganic clay content.

incorporation of clay in SAN or ABS further increases the thermal stability.

In general, the formation of a nanocomposite enhances the thermal stability of the sample, but, the relative increase in the mass loss temperature observed upon nanocomposite formation is reduced as the rubber content increases in ABS. For example, T_{50} of SAN/clay is increased by 14 °C compared to that of virgin SAN, while ABS-17R/clay

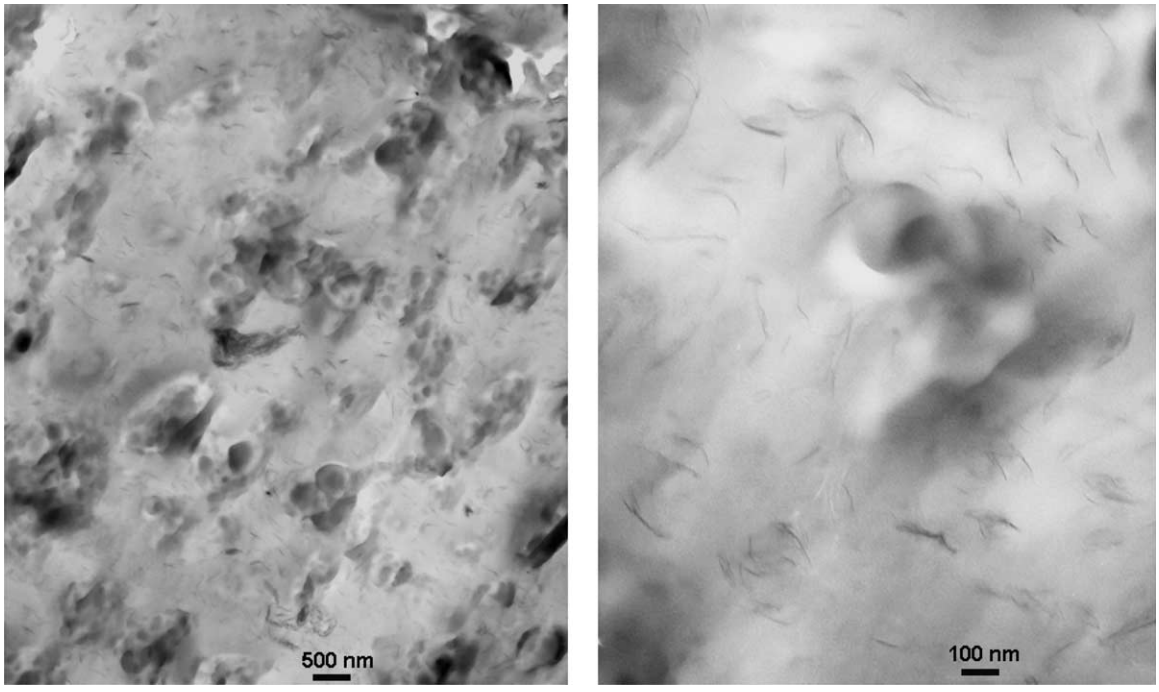

Fig. 3. The TEM images of ABS/10A-clay nanocomposite having 3.0% inorganic clay content at low magnification (left, 10,000×) and high magnification (right, 50,000×).

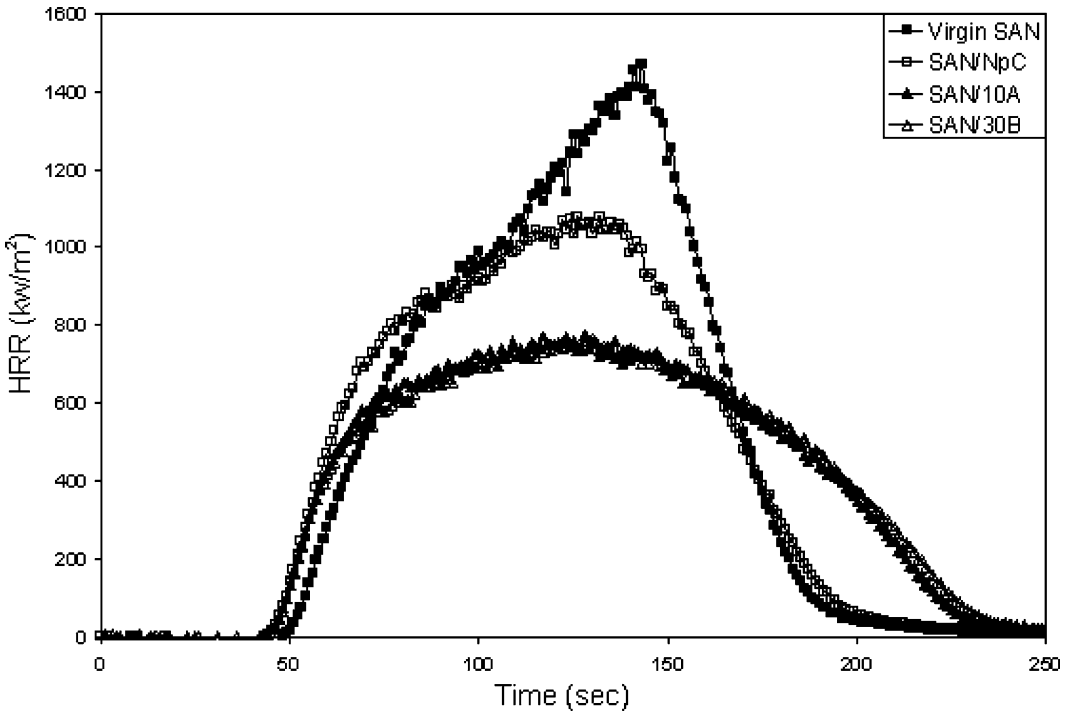

Fig. 4. Cone calorimetry results of virgin SAN and SAN/organically-modified clay nanocomposites (5.0% inorganic clay content).

shows a smaller increase, 9 °C. Considering both the rubber addition and nanocomposite formation for virgin SAN, the temperature at 50% mass loss is increased by 21 °C. It should also be noted that the addition of rubber lead to a slower degradation rate for both virgin polymers and their clay nanocomposites. It is apparent that the thermal stability of ABS and ABS nanocomposites is increased not only because of the well-dispersed clay but also because of the presence of butadiene rubber. It should be noted that previous work [20,21] has shown that the presence of the rubber phase decreases the onset temperature of the degradation. In this study, the temperature at which 10%

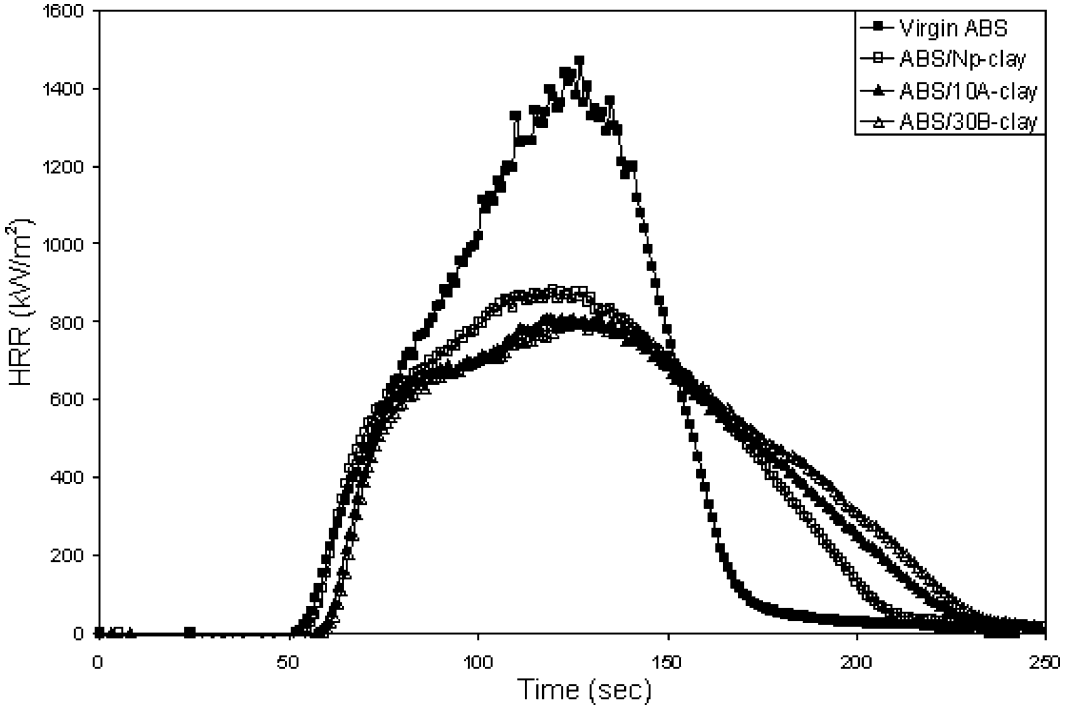

Fig. 5. Cone calorimetry results of virgin ABS and ABS/organically modified clay nanocomposites (5.0% inorganic clay content).

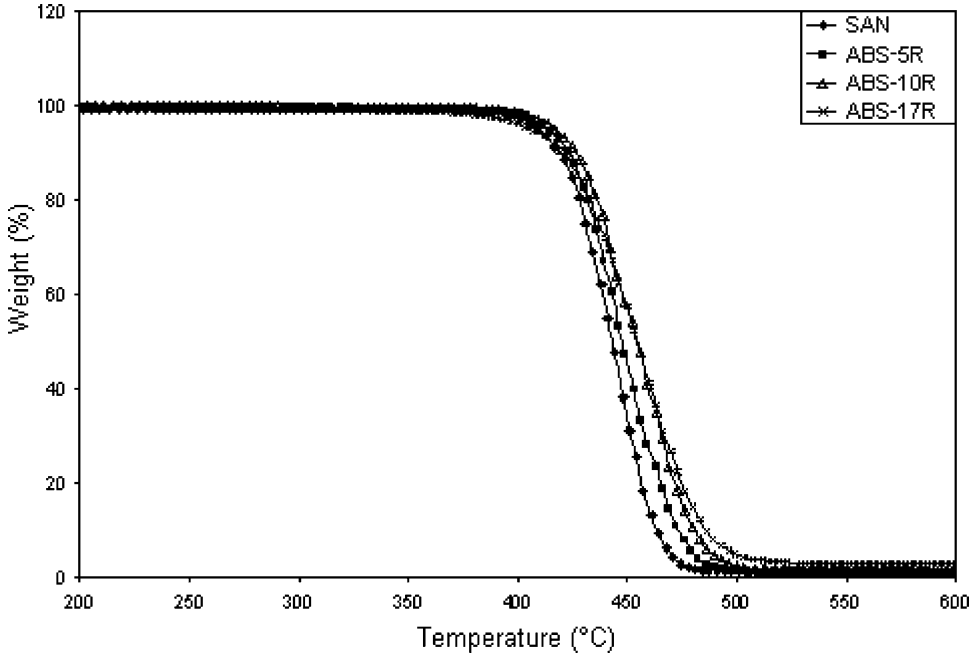

Fig. 6. TGA curves for SAN and ABS having different rubber content.

degradation occurs is used as the onset temperature and these are almost the same within experimental error. Since the acrylonitrile content increases as the butadiene content decreases, this change in acrylonitrile content may also have an impact on the change in thermal stability. Tiganis et al. [31] have reported that aging of ABS has an effect on the thermal stability and the samples used herein have varying thermal histories.

Cone calorimetry shows that the presence of the rubber phase has no effect on the heat release rate; the curves are shown in Fig. 8. It is clearly seen that the addition of clay has a significant effect on the heat release rate. The incorporation of clay brings about a 40–50% reduction in peak heat release rate compared to that of virgin SAN and ABS.

3.3. The analysis of the evolved products during thermal degradation

The evolved gas products were characterized using in situ vapor phase FTIR. Fig. 9 shows the vapor phase FTIR

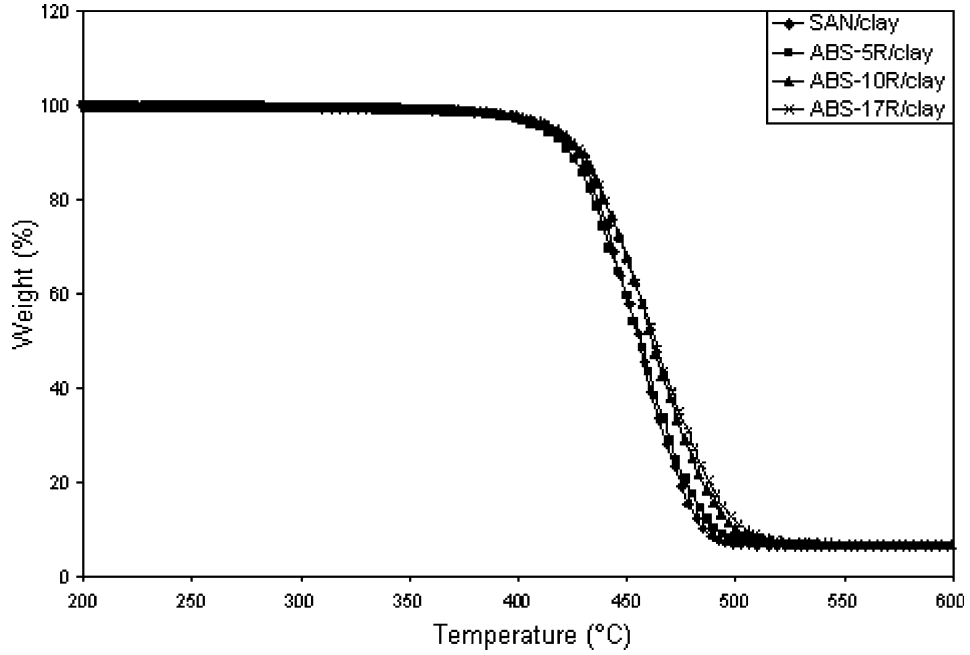

Fig. 7. TGA curves for SAN and ABS nanocomposites.

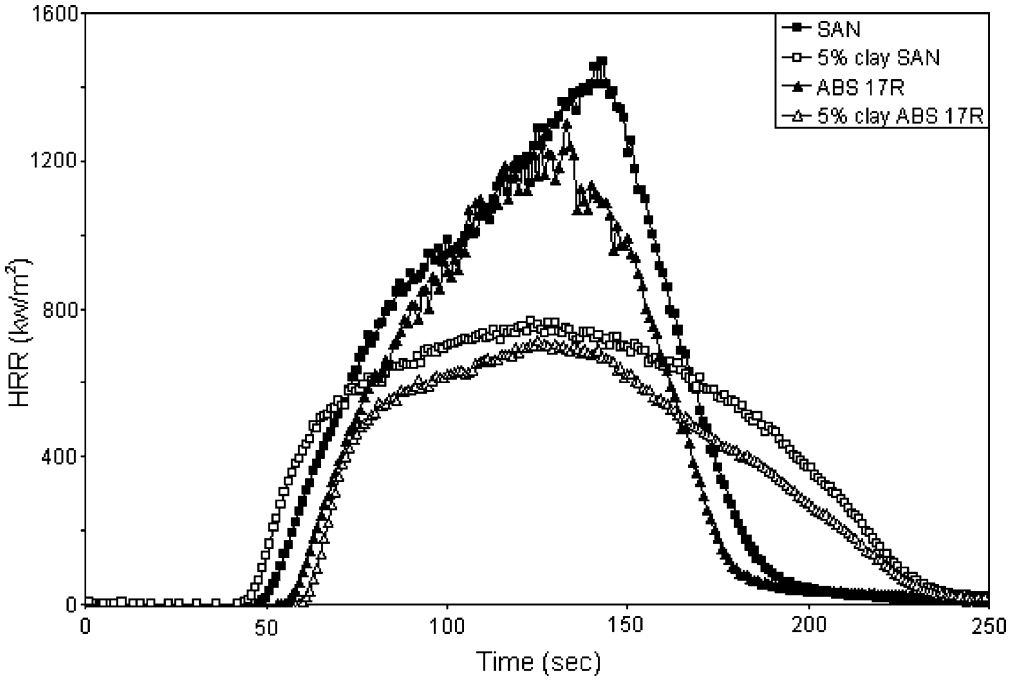

Fig. 8. Cone calorimetry results of SAN, SAN/clay, ABS and ABS/clay.

spectra of SAN, SAN/clay, ABS, ABS/clay at 40% mass loss. In this section, ABS refers to the commercial material, which contains 17% butadiene and has been referred to as ABS-17R previously.

Comparing SAN and SAN/clay, the same FTIR spectra are observed in terms of peak position and relative intensity. ABS and ABS/clay also do not exhibit any changes due to the presence of the clay. This result implies that there are no changes in the evolved products in terms of functionality upon the formation of the nanocomposite. Since ABS contains butadiene rubber, the vapor phase FTIR of ABS and ABS/clay exhibit relatively intense sp^3 carbon–hydrogen stretching bands in the 2800–3000 cm^{-1} region. In the TGA, it was observed that most of the organic portion eventually degrades; probably the rubber phase thermally degrades to aliphatic chains and gives rise to the intense bands in this region.

With the exception of sp^3 carbon–hydrogen stretching modes, all formulations exhibit the same characteristics in the vapor phase FTIR. The bands in the region of 3000–3200 cm^{-1} are caused by sp^2 carbon–hydrogen and the band at 2250 cm^{-1} corresponds to the nitrile group. The

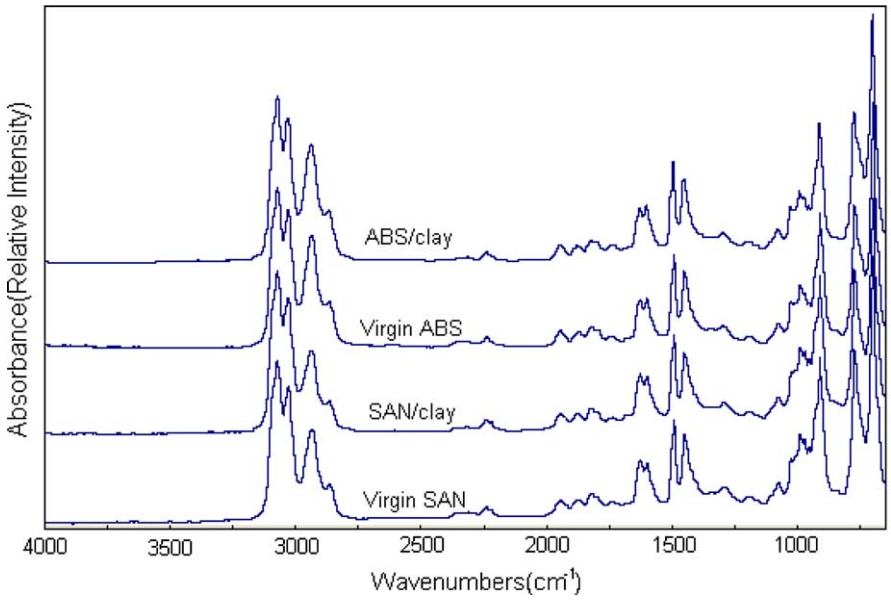

Fig. 9. In situ vapor phase FTIR spectra of SAN, SAN/clay, ABS and ABS/clay at 40% mass loss.

peaks in the region of 1700–2000 and 650–750 cm^{-1} exhibit the diagnostic bands of a mono-substituted benzene ring [32], overtone and combination bands and the out-of-plane carbon–hydrogen deformation, respectively. The band at 1630 cm^{-1} is the carbon–carbon double bond stretching. Through this assignment, the main evolved gas products contain vinyl, nitrile and mono-substituted benzene structures, along with some aliphatic chains.

For structure identification, the evolved products were collected using a cold trap and GC/MS analysis was performed. GC traces of each sample are shown in Fig. 10. The structures were identified through the analysis of mass fragmentation pattern and/or by co-injection with authentic compounds. The assigned structures corresponding to each peak in GC traces are shown in Table 2.

The evolved products can be clearly classified according to the number of monomer units; monomeric structures having either acrylonitrile (AN) or styrene (St) can be identified with GC retention time $<$9.4 min; structures containing both 1AN and 1St unit (*m*/*z* 157, 171, 173) have a retention time of 15.6–17.8 min; those with 2St units (*m*/*z* 196, 208, 222) have a retention time of 19.5–21.6 min; those with 2AN and 1St unit (*m*/*z* 210, 222, 224, 236) have a retention time of 21.7–23.2 min; those with 1AN and 2St units (*m*/*z* 249, 261) have a retention time of 24.5–27.8 min; and 3St units (*m*/*z* 312) show a retention time of 28.4–30.0 min.

No differences are observed between SAN and ABS qualitatively, implying that the same evolved products are formed during thermal degradation of each formulation. In this GC/MS study, only *m*/*z* higher than 50 are seen in the mass spectrum. Considering the in situ vapor phase FTIR results together with GC/MS results of ABS and ABS/clay, it can be speculated that the butadiene rubber degrades to aliphatic chains having small molecular weight that cannot be detected by GC/MS.

When styrene and acrylonitrile are considered as monomer 1 and monomer 2, it was reported that the copolymer reactivity ratios of r_1 and r_2 are 0.35–0.46 and 0.01–0.17 [33]. If r_1 is zero, then monomer 1 must react with monomer 2 in copolymerization, producing an alternating copolymer [34]. Considering the molar ratio and small copolymer reactivity ratio of AN, the probability that AN reacts with another AN is low; the copolymer composition from the AN position is mainly alternating, hence dimers or trimers of acrylonitrile are not expected nor detected in the GC traces. However, since the copolymer reactivity ratio for St is larger than that of AN and the quantity of St used is larger, chain units having adjacent styrene units are possible and the dimer and trimer are detected in small amounts.

Regarding the thermal degradation of virgin SAN, the main evolved products are structures having *m*/*z* 53, 104, 157, 208, 210, 261 and 312. Considering their structures, as shown in Table 2, all have one carbon–carbon double bond in the chain end and an even number of carbons in their chain backbones, implying monomers and oligomers without breaking the carbon–carbon chain of the monomer structure. This result suggests that the evolved compounds

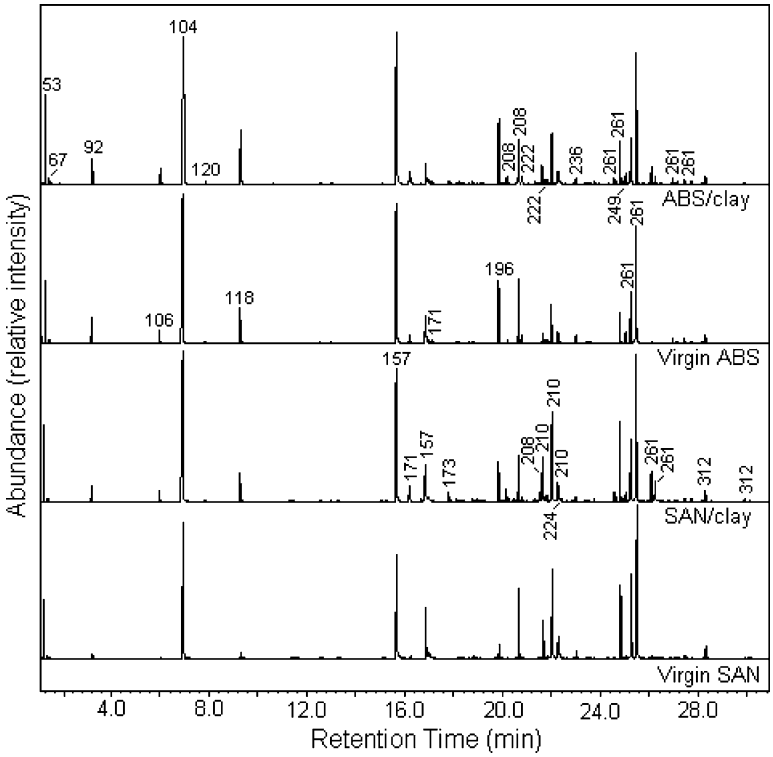

Fig. 10. GC traces for the evolved product of SAN, SAN/clay, ABS and ABS/clay during thermal decomposition. The inset numbers denote the *m*/*z* of the corresponding peak.

Table 2
The structures for the peaks in GC traces

m/z	Time (min)	Structures	*m/z*	Time (min)	Structures
53	1.2	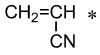	67	1.4	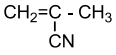
92	3.2		104	6.9	
106	6.1		118	9.4	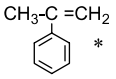
120	7.8	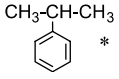	157	15.6, 16.9	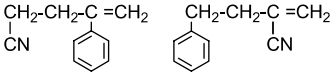
171	16.2, 17.2	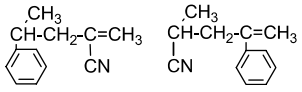	173	17.8	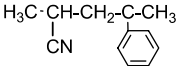
196	19.8	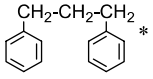	208	20.7	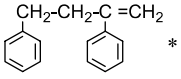
208	20.2, 21.6	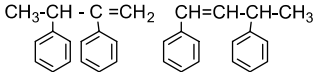	224	22.4	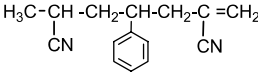
210	21.7, 22.1, 22.3	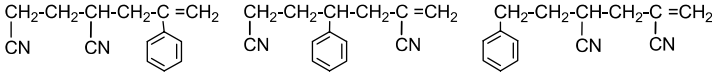			
222	20.8, 21.8	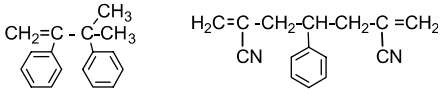			
236	23.2	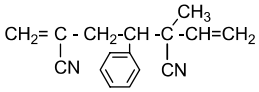	249	25.0	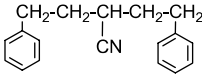
261	24.8, 25.3, 25.5	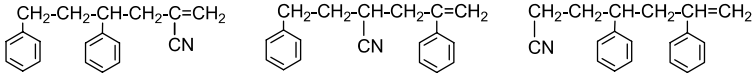			
261	24.5, 26.1, 26.2, 27.0, 27.8	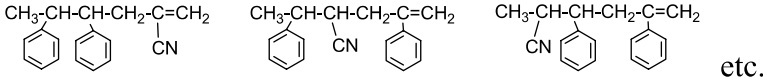 etc.			
312	28.4, 30.0	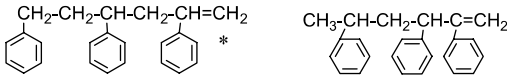			

Structure confirmed by co-injection with authentic compounds.

are produced by β-scission after radical formation by chain scission, as shown in Scheme 1. This is in agreement with the previous work [17–19].

It is assumed that AN is not attached to an AN unit in Scheme 1 and the proposed degradation pathway of SAN is based on the degradation pathway of polystyrene [11]. After the formation of **A** and **B** radicals via chain scission at the '**a**' position, the primary radical **B** is transformed into the tertiary radical **D** because of its increased stability, then α-methyl styrene (*m/z* 118) is produced via β-scission and radical **A** is produced. The **C** radical is produced after acrylonitrile is evolved via β-scission. Hence, the **A** and **C** radicals become the most abundant radicals in the thermal degradation of SAN. These secondary radicals may undergo either β-scission, producing styrene and acrylonitrile, or radical transfer (hydrogen transfer), producing other tertiary radicals. If these tertiary radicals undergo β-scission, then the compounds of *m/z* 157 (dimer), 210 (trimer) and 261 (trimer) are evolved. If chain scission occurs at the '**b**' position in Scheme 1, then 2-cyano-propene (*m/z* 67) is evolved instead of α-methyl styrene and the **A** and **C** radicals are produced in a similar degradation fashion. However, since SAN is not an ideal alternating copolymer, various isomers may be present, as shown in Table 2.

The most prominent difference in the degradation pathways between virgin SAN and virgin PS is in the

relative intensity of monomer(s) in the evolved products. In the case of virgin PS, the dominant evolved product is styrene [12]. For SAN, the monomers are not dominant; the compounds of *m/z* 157, 208, 210 and 261 are also abundant together with monomers. As shown in Scheme 1, the monomers are produced via β-scission by the radicals at the chain ends, while dimers and trimers are evolved via β-scission by the radicals in the middle of chain. In case of the thermal degradation of virgin polystyrene, most abundant radical is the secondary radical adjacent to benzene ring [12], which is one of stable radicals [35,36], hence, most of them undergo β-scission at chain ends rather than radical transfer, producing styrene monomer. On the other hand, one of abundant radicals in the degradation of virgin SAN is the secondary radical adjacent to nitrile group, which is not stable radical, hence considerable amount of these radicals undergoes radical transfer (hydrogen transfer) followed by β-scission, producing various dimers and trimers.

In the presence of clay, some differences are found in the GC traces. First, the relative intensities of the compounds having *m/z* 92, 118, 120, 171, 173, 224 and 249 become significant. All these compounds contain an odd number of carbons in their backbones. The structures of odd carbon number in chain backbone are produced by a different pathway from those of even carbon number which are produced via β-scission from the radical center. It is thought that these odd carbon number chains are produced via extensive random chain scission, as shown in Scheme 2. Due to the formation of the clay nanocomposite and the barrier effect of clay layer, extensive random scission occurs, followed by disproportionation or hydrogen abstraction. Because the degrading polymer chains are confined within the well-dispersed clay layers for some time without evolving, they may experience superheated conditions in the TGA, leading to extensive random chain scission at any methylene linkage in the presence of clay. The even carbon number compounds can be produced via extensive random scission, but only the odd number carbon compounds are expressed in this scheme. Since SAN is not a perfect alternating copolymer and the mol% of styrene is larger, there are some styrene units connected to other styrene units and this lead to the evolution of 1,3 diphenylpropane (*m/z* 196) following the extensive random scission as shown in Scheme 2.

The second difference between virgin polymers and nanocomposites is found in the number of isomers. In virgin SAN and ABS, there are three significant peaks for *m/z* 261 corresponding to head-to-tail structures (retention times 24.8, 25.3, and 25.5 min), as shown in Table 2. In the

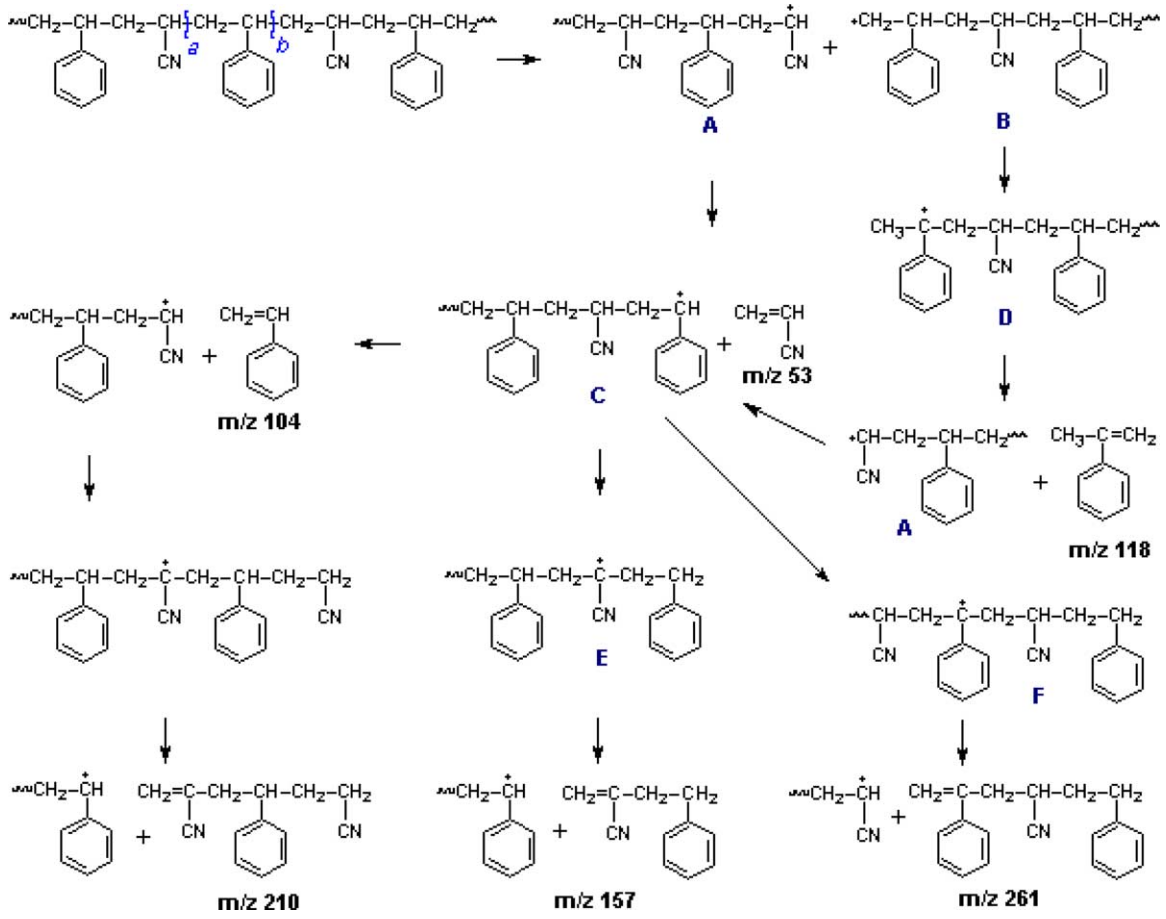

Scheme 1. Thermal degradation pathway of virgin SAN.

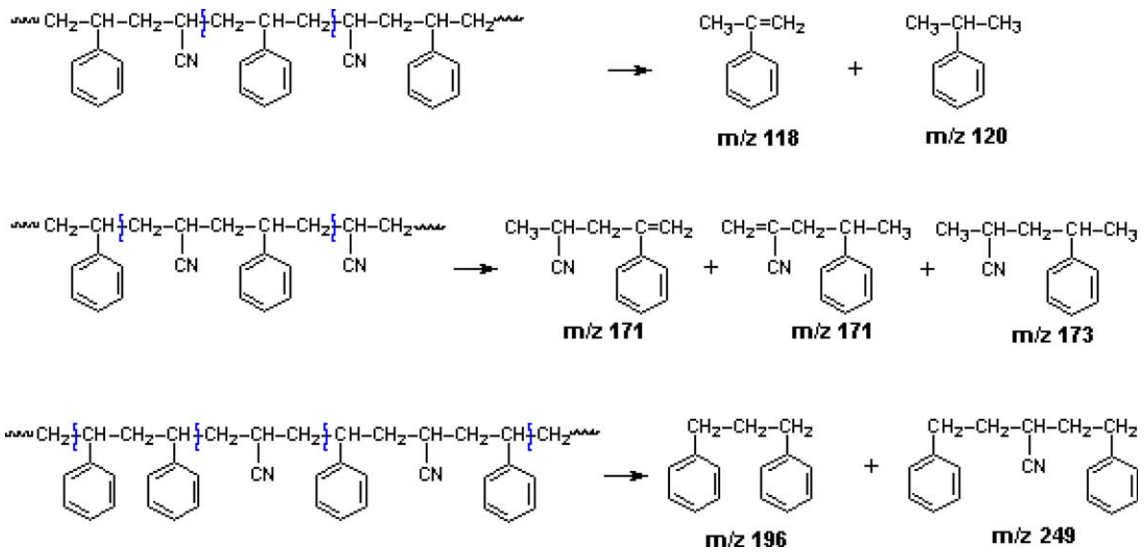

Scheme 2. Extensive random scission of SAN in the presence of clay.

presence of clay, five more *m*/*z* 261 peaks are detected; these are thought to be head-to-head structures which are speculatively assigned, as shown in Table 2. Some additional head-to-head structures are assigned in the compounds of *m*/*z* 208, 222 and 236. These head-to-head structures are produced via radical recombination reactions followed by random scission due to the barrier effect of the clay in a similar reaction fashion as that of polystyrene [12]. However, the abundance of head-to-head structures during the thermal degradation of SAN is much smaller than for PS. This trend may be caused by differences in the radical stability between degrading SAN and PS. The only tertiary radical in the degradation PS is adjacent to a benzene ring, the '**F**' type radical in Scheme 1, whereas SAN has both radicals adjacent to a nitrile, '**E**' in Scheme 1, and that adjacent to a benzene ring. In terms of radical stability, the tertiary radical adjacent to benzene ring is more stable than that to nitrile [35,36], hence, as soon as radical '**E**' is produced, it undergoes either radical transfer (hydrogen transfer) or β-scission, producing relatively large amount of dimers and trimers compared to polystyrene. On the other hand, the radical adjacent to benzene ring is one of the more stable radicals [35,36], so it has more opportunity to undergo recombination reaction. Polystyrene produces the only '**F**' type radicals, leading to a considerable number of head-to-head structures in the presence of clay due to the recombination reaction caused by the clay barrier.

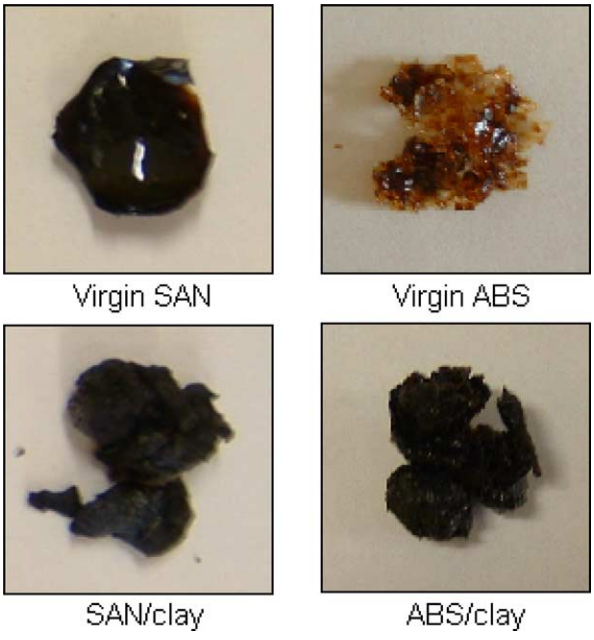

Fig. 11. Residues of SAN, SAN/clay, ABS and ABS/clay after 40% mass loss.

If one compares the GC trace of virgin SAN with that of virgin ABS, the ABS trace includes more intense peaks at *m*/*z* 92, 118, 171 and 196. These compounds have an odd number of carbons in their backbones, which are evolved via extensive random scission, as shown in Scheme 2. It can be speculated that butadiene rubber acts as a physical barrier to cause extensive random scission in the SAN phase, which may explain why higher thermal stability of ABS is shown in the TGA. However, the butadiene rubber eventually undergoes thermal degradation, producing short aliphatic chains, so it does not provide the environment for degrading SAN phase to undergo radical recombination reaction as the well-dispersed clay does.

Summarizing the effect of clay on the degradation of SAN, two additional degradation pathways are introduced by the formation of the nanocomposite leading to better thermal stability and fire retardancy; extensive random scission and radical recombination through the barrier effect of the clay. These results are very comparable to that seen in polystyrene/clay nanocomposite [12].

3.4. Solid residue samples after 40% mass loss

In order to see the changes in the condensed phase during decomposition, the residues after 40% mass loss were collected. The color of the residues becomes dark and the luster of the surface is reduced by clay addition, as shown in Fig. 11. Comparing the residue of virgin SAN with that of virgin ABS, SAN exhibits a smooth surface, while ABS has a rough surface, implying that the butadiene rubber phase in ABS impedes the flow of the SAN phase, supporting the physical barrier effect of the rubber phase as described in the previous section. The residues of SAN/clay and ABS/clay maintain their shapes and the surfaces become hard and strong enough to form an insulating surface layer.

4. Conclusion

The degradation pathway of SAN and ABS, in general, follows the same degradation pathway as described for polystyrene; chain scission followed by β-scission (depolymerization). In the presence of clay, two additional reactions, radical recombination reactions and extensive random scission, become significant as the clay content increases. Since ABS shows a well-dispersed morphology with a separate phase of butadiene rubber in the SAN matrix, the evolved products in the degradation of ABS are not different from those of SAN copolymer. The effect of rubber is similar to that of the clay, but not as effective due to its shorter duration. The difference in the degradation pathways of virgin SAN and virgin PS is in the evolution of dimers and trimers; SAN shows more evolution of these dimers and trimers, implying more radical transfer followed by β-scission. In the presence of clay, SAN nanocomposite produces smaller amount of recombined products compared PS nanocomposite, probably because the tertiary radical of the acrylonitrile unit is less stable than the corresponding styryl radical.

References

[1] Kojima Y, Usuki A, Kawasumi M, Okada A, Fukushima Y, Karauchi T, et al. J Polym Sci, Part A: Polym Chem 1993;31:983–6.
[2] Okada A, Kawasumi M, Kurauchi T, Kamigaito O. Polym Prepr 1987; 28:447–8.
[3] Kojima Y, Usuki A, Kawasumi M, Okada A, Kurauchi T, Kamigaito O. J Polym Sci, Polym Chem 1993;31:1755–8.
[4] Kojima Y, Usuki A, Kawasumi M, Okada A, Kurauchi T, Kamigaito O. J Appl Polym Sci 1993;49:1259–64.
[5] Bourbigot S, Gilman JW, Wilkie CA. Polym Degrad Stab 2004;84: 483–92.
[6] Kojima Y, Usuki A, Kawasumi M, Okada A, Kurauchi T, Kamigaito O. J Polym Sci, Polym Chem 1993;31:983–6.
[7] Zhu J, Morgan AB, Lamelas FJ, Wilkie CA. Chem Mater 2001;13: 3774–80.
[8] Bourbigot S, Gilman JW, Wilkie CA. Polym Degrad Stab 2004;84: 483–92.
[9] Alexandre M, Dubois P. Mater Sci Eng 2000;R28:1–63.
[10] Ray SS, Okamoto M. Prog Polym Sci 2003;28:1539–641.
[11] Gilman JW, Jackson CL, Morgan AB, Harris Jr R, Manias E, Giannelis EP, et al. Chem Mater 2000;12:1866–73.
[12] Jang BN, Wilkie CA. Polymer 2005;46:2933–42.
[13] Jang BN, Wilkie CA. Polymer 2005;46:3264–74.
[14] Costache M, Wilkie CA. Polym Mater Sci Eng 2004;91:30–1.
[15] Chen K, Susner MA, Vytazovkin S. Macromol Rapid Commun 2005; 26:690–5.
[16] Vanderhart DL, Bourbigot S, Gilman J, Bellayer S, Stretz H, Paul DR. In: Le Bras M, Wilkie CA, Bourbigot S, editors. Fire retardancy of polymers; new trends in using halogen-free mineral additives and fillers. UK: Royal Society of Chemistry; 2005. p. 203–13.
[17] Grassie N, Bain DR. J Polym Sci, Part A-1 1970;8:2653–64.
[18] Grassie N, Bain DR. J Polym Sci, Part A-1 1970;8:2665–77.
[19] Grassie N, Bain DR. J Polym Sci, Part A-1 1970;8:2679–88.
[20] Luda di Cortemiglia MP, Camino G, Costa L, Guaita M. Thermochim Acta 1985;93:187–90.
[21] Suzuki M, Wilkie CA. Polym Degrad Stab 1995;47:217–21.
[22] Shapi MM, Hesso A. J Chromatogr 1991;562:681–96.
[23] Bourbigot S, Vanderhart DL, Gilman JW, Bellayer S, Stretz H, Paul DR. Polymer 2004;45:7627–38.
[24] Chigwada G, Jiang DD, Wilkie CA. In: Wilkie CA, Nelson GL, editors. Fire and polymers IV: Materials and concepts for hazard prevention. ACS Symp. Ser 922, Oxford: Oxford University Press; 2005. pp. 103–16.
[25] Jang BN, Wang D, Wilkie CA. Macromolecules 2005;38:6533–43.
[26] Gilman JW, Kashiwagi T, Nyden M, Brown JET, Jackson CL, Lomakin S, et al. In: Al-Maliaka S, Golovoy A, Wilkie CA, editors. Chemistry and technology of polymer additives. London: Blackwell Scientific; 1998. p. 249–65.
[27] Zanetti M, Camino G, Canavese D, Morgan AB, Lamelas FJ, Wilkie CA. Chem Mater 2002;14:189–93.
[28] Bourbigot S, Vanderhart DL, Gilman JW, Bellayer S, Stretz H, Paul DR. Polymer 2004;45:7627–38.
[29] Stretz HA, Wootan WL, Cassidy PE, Koo JH. Polym Mater Sci Eng 2004;91:94–5.
[30] Echte A. In: Riew CK, editor. Rubber-toughened plastics. Washington, DC: American Chemical Society; 1989 [chapter 2].
[31] Tiganis BE, Burn LS, Davis P, Hill AJ. Polym Degrad Stab 2002;76: 425–34.
[32] Socrates G. Infrared and raman characteristic group frequencies. New York: Wiley; 2001 [chapters 2 and 3].
[33] Fouassier JP. In: Brandrup J, Ummergut EH, Grulke EA, editors. Polymer handbook, 4th ed, New York: Wiley; 1999. p. II, 251.
[34] Odian G. Principles of polymerization. 3rd ed. New York: Wiley; 1991. p. 454–76.
[35] Fossey J, Lefort D, Sorba J. Free radicals in organic chemistry. New York: Wiley; 1995. p. 31–8.
[36] March J. Advanced organic chemisty. New York: Wiley; 1992. p. 186–93.